Electronic Supplementary Material (ESI) for Physical Chemistry Chemical Physics.

Electronic Supplementary Information:

Diffusional transport to and through thin-layer nanoparticle film modified electrode: CdSe nanoparticle modified electrodes

William G. Hepburn, Christopher Batchelor-McAuley, Kristina Tschulik, Edward O. Barnes, Roohollah Torabi Kachoosangi[+], Richard G. Compton*

Department of Chemistry, Physical and Theoretical Chemistry Laboratory, University of Oxford, South Parks Road, Oxford OX1 3QZ, United Kingdom

[+]now at; C-Tech Innovation Ltd, Capenhurst Technology Park, Chester, CH1 6EH, United Kingdom

Section 1: The effect of film thickness on our rate constant

The variation of $k_{Red,App}$ (red line) and $k_{Ox,App}$ (blue line) as a function of the overpotential (V) and the film thickness (x_f = 0.1, 1, 10, 100nm). Other parameters; k_0 = 0.01 m s^{-1}, $K_A = K_B$ = 0.1, $D_{A,f} = D_{B,f} = 1x10^{-10}$ m^2 s^{-1}, α = β = 0.5.

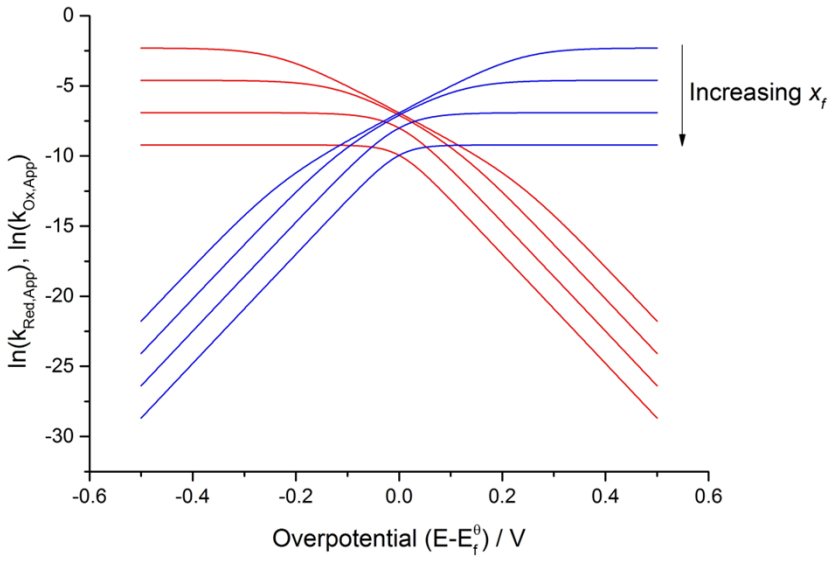

Section 2: Theoretical Model

The cyclic voltammetry of a redox couple A/B is simulated:

$A + e^- \rightleftharpoons B$ Equation 1

The reduction takes place at a macrodisc electrode, hence the mass transport may be modelled using Fick's second law in linear space:

$$\frac{\partial[i]}{\partial x} = D_{i,s}\frac{\partial^2[i]}{\partial x^2}$$ Equation 2

where $[i]$ is the concentration of species i (mol m^{-3}), x is the distance from the electrode surface (m) and $D_{i,s}$ is the diffusion coefficient (in solution, as opposed to in the film) of species i (m^2 s^{-1}). A large excess of inert, fully dissociated supporting electrolyte is assumed to be present in solution, ensuring that diffusion is the only form of mass transport present.

Equation 2 must be solved subject to appropriate boundary conditions. Boundaries are set at $x = x_f$, the location of the edge of the film covering the electrode (see main text) and at $x = 6\sqrt{D_{max}t_{max}}$, a position well outside the diffusion layer[1, 2], providing $x_f \ll 1$ (D_{max} and t_{max} are respectively the largest diffusion coefficient in the system and the total time of the experiment).

At the bulk solution boundary, a zero flux condition is imposed on both species:

$$\left(\frac{\partial[i]}{\partial x}\right)_{6\sqrt{D_{max}t_{max}}} = 0$$ Equation 3

At $x = x_f$, the outer edge of the thin film, we apply a modified form of the Butler-Volmer equation, as derived in the main text, as the boundary condition for species A:

$$D_{A,s}\left(\frac{\partial[A]}{\partial x}\right)_{x_f,s} = \frac{k_0\left(K_A[A]_{x_f,s}e^{-\propto\theta} - K_B[B]_{x_f,s}e^{\beta\theta}\right)}{1 + k_0 x_f\left(\frac{1}{D_{A,f}}e^{-\propto\theta} + \frac{1}{D_{B,f}}e^{\beta\theta}\right)}$$ Equation 4

where a subscript *s* indicates a value in the solution, and a subscript *f* indicates a value in the film. K_i is a partition ratio, and is given by:

$$K_i = \frac{[i]_{x_f,f}}{[i]_{x_f,s}}$$ Equation 5

Conservation of mass is used as the boundary condition for species B at x_f:

$$D_{B,s}\left(\frac{\partial[B]}{\partial x}\right)_{x_f,s} = -D_{A,s}\left(\frac{\partial[A]}{\partial x}\right)_{x_f,s}$$ Equation 5

A series of dimensionless parameters are introduced to simplify the model by reducing the number of independent parameters and removing scaling factors such as concentration. These are listed in Table 1. Upon introduction of these parameters, the mass transport equation becomes:

$$\frac{\partial C_i}{\partial X} = D_i' \frac{\partial^2 C_i}{\partial X^2}$$ Equation 6

The bulk solution boundary conditions become:

$$\left(\frac{\partial [i]}{\partial x}\right)_{6\sqrt{D_{max}' \tau_{max}}} = 0$$ Equation 7

And the film surface boundary conditions become:

$$\left(\frac{\partial C_A}{\partial X}\right)_{X_f,s} = \frac{K_0\left(K_A C_{A,x_f,s} e^{-\propto\theta} - K_B C_{B,x_f,s} e^{\beta\theta}\right)}{1 + K_0 X_f \left(\frac{1}{D_{A,f}'} e^{-\propto\theta} + \frac{1}{D_{B,f}'} e^{\beta\theta}\right)}$$ Equation 8

$$D_{B,s}' \left(\frac{\partial C_B}{\partial X}\right)_{X_f,s} = -\left(\frac{\partial C_A}{\partial X}\right)_{X_f,s}$$ Equation 9

Initial conditions are $C_A = 1$ and $C_B = 0$ everywhere. At the start of the experiment, $\tau = 0$, an initial potential θ_i is applied to the electrode, and varies with dimensionless time according to the equation:

$$\theta = |\theta_i - \theta_v - \sigma\tau| + \theta_v$$ Equation 10

where θ_v is the vertex potential and σ is the dimensionless scan rate.

The dimensionless current is then calculated at all times as:

$$j = -\left(\frac{\partial C_A}{\partial X}\right)_{X_f,s}$$ Equation 11

This is made converted to a real current according to:

$$I = 2\pi F D_{A,s} [A]^* r_e j$$ Equation 12

where F is Faraday's constant (=96485 C mol^{-1}), $[A]^*$ is the bulk concentration of species A (mol m^{-3}), and r_e is the electrode radius (m).

Equations 6-9 and 11 were discretised according to the Crank-Nicolson method[3] and implicitly solved simultaneously over an exponentially expanding spatial grid using the Thomas Algorithm.[4] Previously defined spatial and temporal grids were used,[5, 6] which were found to produce results within 0.2% of a fully converged result. The model was programmed

in C++ and run on an Intel® Core™2 Duo 2.99 GHz PC with 3.5 GB RAM. Typical simulation times were 5-10 s.

Parameter	Definition
C_i	$\frac{[i]}{[A]}$
$D_i^{'}$	$\frac{D_i}{D_A}$
K_0	$\frac{r_e k_0}{D_A}$
θ	$\frac{F(E - E_f)}{RT}$
σ	$\frac{Fr_e^2 \upsilon}{RTD_A}$
X	$\frac{x}{r_e}$

Table 1: Definitions of dimensionless parameters used in this study

Section 3: Nanoparticle Characterisation

The CdSe nanoparticles (CANdots® Series A, CAN GmbH, Hamburg) were characterised by dynamic light scattering (Malvern Instruments Ltd, UK) and fluorescence spectroscopy. The measured diameter of 34 ± 6nm agrees as an approximation with the suppliers 28nm value used in this work. The fluorescence emission spectrum was carried out on a Carry Eclipse Spectrophotometer (Varian, Australia) and shows a maximum at wavelength 530nm agreeing exactly with the supplier.

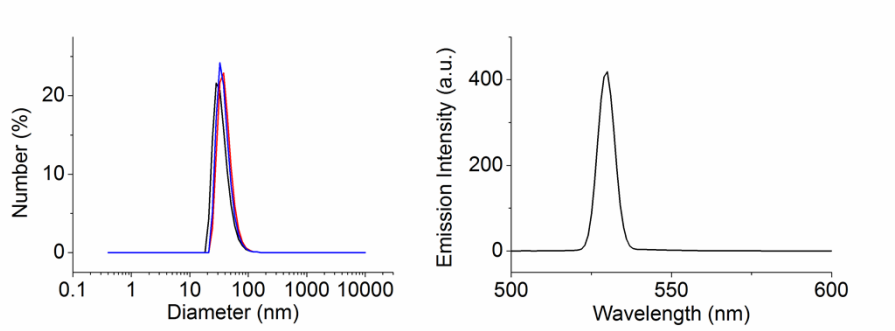

Section 4: Ruthenium Kinetics on Gold

The kinetics of ruthenium (III) hexaamine has been well studied on gold electrodes. Experiments carried out agree with other literature investigations. In the absence of a film on the electrode a linear dependence of peak current with scan rate is observed. The peak potential also remains constant. This differentiates the kinetics from those observed in figure 5 with the organic film on our electrode.

Voltammetry of 1 mM $Ru(NH_3)_6Cl_3$ in 0.1 M Na_2SO_4 0.02 M H_3BO_3 0V to -0.4V on a gold macroelectrode with scan rates range from 0.01 to 1.6 Vs^{-1}.

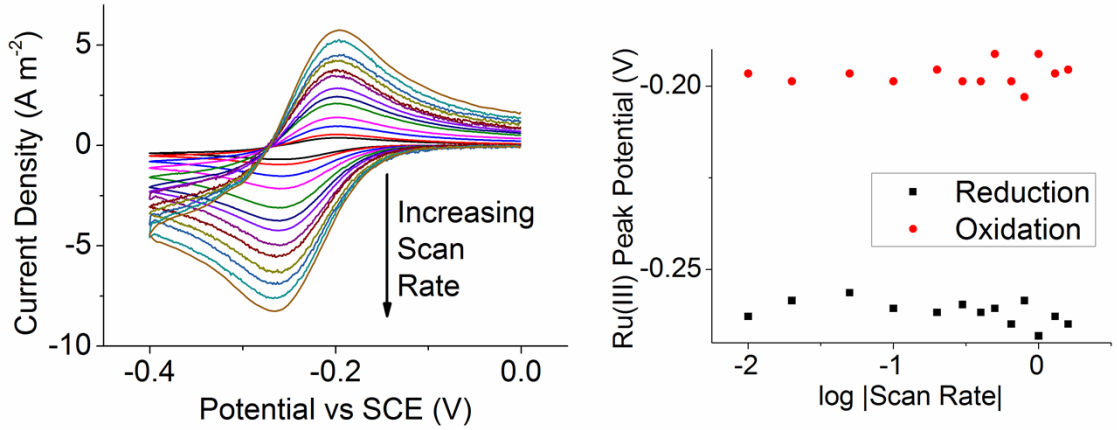

Section 5: Dependence of cathodic peak on boric acid

Figure 10 (main article) demonstrates a cathodic peak observed at -1.41V vs SCE. The magnitude of this peak varies linearly with the boric acid concentration in agreement with the Randles-Ševčík equation identifying the involvement of boric acid in the electrochemical process (as shown in the figure below).

Voltammetry of H_3BO_3 in 0.1M Na_2SO_4 0V to -1.6V at scan rate 0.05V s^{-1} on a gold macroelectrode modified with 5 monolayers of organic capped CdSe nanoparticles. Concentrations of H_3BO_3 are 0.005, 0.01, 0.02, 0.03M.

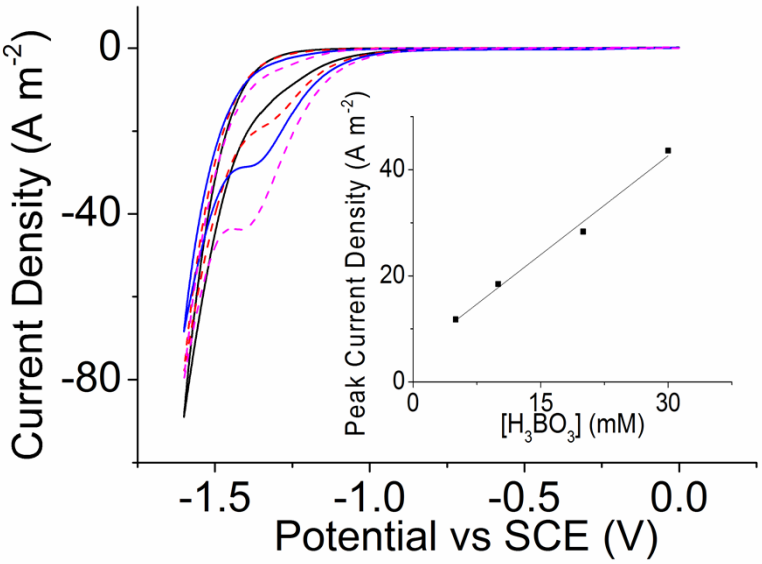

References

1. D. J. Gavaghan, *J. Electroanal. Chem.*, 1998, 456, 13-23.
2. D. Britz, *Digital simulation in electrochemistry*, Springer-Verlag, 1988.
3. J. Crank and P. Nicolson, *Proc. Camb. Phil. Soc.*, 1947, 43, 50-67.
4. W. H. Press, S. A. Teukolsky, W. T. Vetterling and B. P. Flannery, *Numerical Recipies in C*, 1992.
5. E. O. Barnes, S. R. Belding and R. G. Compton, *J. Electroanal. Chem.*, 2011, 660, 185-194.
6. E. O. Barnes, Y. Wang, J. G. Limon-Petersen, S. R. Belding and R. G. Compton, *J. Electroanal. Chem.*, 2011, 659, 25-35.